Fire Technology (2025) 61:2957–2998
https://doi.org/10.1007/s10694-025-01711-3

Evaluating Fire Severity in Electric Vehicles and Internal Combustion Engine Vehicles: A Statistical Approach to Heat Release Rates

Mohd Zahirasri Mohd Tohir[1,2] · **César Martín-Gómez**[1]

Received: 29 April 2024 / Accepted: 26 January 2025 / Published online: 12 February 2025

Abstract
This study provides a comprehensive statistical analysis of heat release rate (HRR) profiles in electric vehicles (EVs) and internal combustion engine (ICE) vehicles, addressing fire safety challenges in performance-based design. Using experimental data, key parameters such as peak heat release rate (PHRR), time to peak heat release rate (TPHRR), total heat released (THR), and growth coefficients were analysed. Results reveal that EVs, exhibit distinct fire dynamics, often displaying higher PHRR values than ICE vehicles, which highlights the potential for greater fire intensity and growth rates in EV fires. A design fire model was constructed based on this analysis, offering fire engineers a probabilistic alternative to conventional deterministic approaches for simulating vehicle fire scenarios in various infrastructural contexts. This probabilistic approach provides a more flexible framework for decision-making in fire risk assessments. Additionally, the study observed a correlation between larger battery sizes and increased fire severity in EVs, though this should be interpreted cautiously given the limited dataset. This work highlights the importance of adapting fire safety standards to keep pace with advancements in vehicle technology, especially with the growing prevalence of EVs. Future research should aim to expand the dataset with more diverse experiments to enhance the robustness of design fire models, supporting the development of tailored fire safety strategies for different vehicle types across various environments.

Keywords Electric vehicle · Combustion vehicle · Heat release rate · Statistics · Experimental data

Abbreviations

BEV	Battery electric vehicle
DP	Date published
ED	Experiment date

✉ Mohd Zahirasri Mohd Tohir
zahirasri@upm.edu.my

[1] Department of Construction, Building Services and Structures, Universidad de Navarra, Pamplona, Spain

[2] Safety Engineering Interest Group (SEIG), Department of Chemical and Environmental Engineering, Universiti Putra Malaysia, 43400 Serdang, Selangor, Malaysia

EV	Electric vehicle
EVs	Electric vehicles
FCEV	Fuel cell electric vehicle
HRR	Heat release rate
ICE	Internal combustion engine
kW	Kilowatts
kWh	Kilowatt-hours
LMO	Lithium-ion manganese oxide
LiB	Lithium-ion battery
MJ	Mega joules
NMC	Nickel manganese cobalt
PHEV	Plug-in hybrid electric vehicle
PHRR	Peak heat release rate
RS	Report submitted
THR	Total heat released
TPHRR	Time to reach Peak HRR

1 Introduction

Performance-based design in fire safety engineering is increasingly crucial [1], especially with the integration of new technologies like Electric Vehicles (EVs) and their infrastructure. This approach focuses on establishing clear objectives and performance criteria, allowing for a tailored response to specific challenges and risks, such as those posed by EV charging stations and energy storage systems in buildings. The concept of the design fire, central to performance-based building design, is particularly vital in the context of assessing the fire safety risks associated with EVs compared to traditional internal combustion vehicles [2]. The design fire is characterized by its heat release rate (HRR), a measure of the intensity and growth of a fire over time [3]. This parameter becomes important when evaluating the fire hazards posed by EVs, as their battery systems can potentially lead to different fire behaviours compared to conventional vehicles.

The uncertainty surrounding EV fires, particularly in settings like car parks whether on the surface or underground, poses a significant challenge in the realm of performance-based design [4]. Unlike fires in internal combustion engine (ICE) vehicles, the behaviour of EV fires is less understood, raising questions about their intensity, the speed of fire spread, and their interaction with other combustibles in close proximity [5, 6]. This lack of quantified information complicates the task of accurately determining the HRR for design fires in EV scenarios.

Over recent years, numerous isolated fire tests on EVs have provided valuable insights [7], yet a collective statistical understanding of how EVs perform in fire scenarios compared to ICE vehicles remains elusive. While these tests have yielded conclusions specific to their objectives, they do not paint a comprehensive picture of EV fire behaviour on a larger scale. In contrast to ICE vehicles, where fire characteristics are more established as compared to EVs, the varying battery technologies and configurations in EVs may potentially lead to a diverse range of fire behaviours. This variability adds complexity to the already challenging task of defining the HRR for EV fires, necessary for performance-based design in environments like car parks. The limited statistical aggregation of EV fire

data hinders the ability to draw definitive comparisons between EV and ICE vehicle fires, particularly in terms of intensity, spread rate, and interaction with nearby combustibles.

Addressing these challenges, it is noteworthy that currently, there exists no comprehensive research that has systematically gathered information about the HRR profiles for EV fires from various tests. This gap in research forms the primary objective of this work. The aim is to compile and analyse HRR profiles of EV fires, exclusively drawing from available laboratory experiment results which provide sufficient explanations of the tests and experiments. This focused approach, relying solely on laboratory data, ensures a controlled and consistent source of information for analysis, thereby contributing to a more accurate and reliable understanding of the HRR characteristics specific to EV fires.

Through a thorough analysis of HRR profiles, this work aims to develop a more comprehensive understanding of fire dynamics specific to EVs. The analysis will encompass not only the peak heat release rates but also the duration, growth rate, and decay phase of EV fires, with a particular emphasis on the growth aspect. This data will subsequently be compared with the HRR profiles of ICE vehicles, which have undergone more extensive analysis in the past [2, 8, 9]. Such a comparison is vital for identifying both differences and similarities in fire behaviour between EVs and ICE vehicles, providing valuable insights into the distinct fire risks and characteristics associated with each type of vehicle.

This work is expected to provide invaluable insights for fire engineers, particularly in designing safer car parks, by offering a detailed comparison of HRR profiles in EV and ICE vehicle fires. A central aim of this study is to equip fire engineers with an alternative approach for simulating vehicle fire scenarios. By incorporating probabilistic design fire inputs, this research provides engineers with options beyond conventional deterministic methods, allowing for more flexible and informed decision-making in fire safety strategies and infrastructure design. These insights are crucial for advancing fire safety practices, particularly in car park settings where the distinct fire behaviours of EVs and ICE vehicles must be carefully considered.

2 Material and Methods

The heat release rate curves for single passenger electric vehicles have been sourced from various publications detailing large-scale calorimeter fire experiments conducted between the 2010s and the early 2020s. This work is confined to single EVs, as data from experiments involving other vehicle scenarios are scarce. The primary focus of this analysis lies in examining three key characteristics discernible from the heat release rate curves: the peak heat release rate, the time to reach peak heat release rate, and the total energy released during the combustion process.

While there is some overlap with prior research, particularly in the realm of designing EV fires as explored by researchers such as Sun et al. [6], Hynynen et al. [10], Boehmer et al. [11], and Dorsz and Lewandowski [7], this current study diverges in its approach. Previous studies have not explored into a statistical analysis of severity characteristics associated with EV fires especially during the growth stage, and this work includes recent experiments conducted such as Kang et al. and Willstrand et al. [12, 13] that were not previously considered.

To fulfil the objectives of this work, two main components are presented. The first involves a comprehensive collation and summary of single EV fire experiments, including a detailed reproduction of the heat release rate curves from these experiments. The second

component is a distribution analysis, which compiles the experimental data and proposes a distribution shape for each identified burning severity characteristic.

However, to enable meaningful comparisons with ICE vehicles, an update to the single passenger ICE vehicle fire experiment database is necessary. The most recent distribution data for ICE vehicles dates back to 2013, from the work of Tohir and Spearpoint [9]. Therefore, this work also incorporates a data collection effort for ICE vehicles, focusing on literature published post the Tohir and Spearpoint study. This step is key given that, over the years, the materials used inside vehicles have evolved, featuring different material compositions. Understanding these changes is essential for accurate comparisons and analyses of fire characteristics between EVs and ICE vehicles. This dual approach, involving both EV and updated ICE vehicle data, ensures a comprehensive and current understanding of vehicle fire dynamics.

2.1 Experimental Data Gathering

A total of 16 single EV fire experiments and 17 single ICE vehicle fire experiments have been collated, with details sourced from corresponding reference materials (Table 1). The gathered information for both EVs and ICE vehicles is systematically presented in a comprehensive table format. For detailed specifics on EVs, refer to Table 2, and for ICE vehicles, see Table 3.

These tables includes a unique identifier for each vehicle, specifying the types of EV or ICE vehicle, the battery capacity in the EVs during the test, the state of charge of the battery, and the cell type of the battery. Additionally, it provides details about the model and year of manufacture for all vehicles. The table also covers information regarding the fire condition of the vehicles, such as the method used to initiate the fire during experiments i.e., the locations and ignition source of the fires, and the conditions of the vehicles (for example, the state of window openings). Finally, the table describes how the HRRs were measured, a process referred to as 'Heat release rate evaluation method'. This extensive compilation of data aims to provide a clear and detailed overview of each experiment's specifics, encompassing both EVs and ICE vehicles.

Table 1 comprehensively explains each column, detailing critical specifications and conditions relevant to the study of EV and ICE vehicle fires. This includes categories such as EV types—Battery Electric Vehicle (BEV), Plug-in Hybrid Electric Vehicle (PHEV), and Fuel Cell Electric Vehicle (FCEV)—and key parameters like Battery Capacity, State-of-Charge, and Battery Cell Type. For ICE vehicles, specifics such as Fuel Type and Fuel Balance are outlined. Additionally, the table provides insights into the 'Condition' of vehicles prior to ignition, 'Ignition source', and 'Ignition location'. Furthermore, the 'Reference' column contains information about the primary source of the experiment. The column displays the publication date of the resource.

The 'Heat release rate evaluation method' column clarifies how the heat release rate curve was derived from each experiment. However, it's important to note that not all sources provided explicit details on the exact techniques used, so the information in this column is based on the interpretations made from the original publications. Additionally, it is important to acknowledge that the different techniques used to measure heat release rates, such as mass loss rate, convective calorimetry, and species-based calorimetry, may lead to variations in the measurements of heat release rates [14]. This variability can influence the analysis of fire severity. The term 'Mass loss' in this context means that the heat release rate was determined through measuring the mass loss of the vehicle during

Table 1 Explanation about important columns in Table 2

EV types	Battery capacity	Battery state-of-charge, %	Battery cell type	Condition	Ignition location	Ignition source
Detailed descriptions under several specific headers: EV Types categorizes the different powertrain of the EV namely, Battery Electric Vehicle (BEV), Plug-in Hybrid Electric Vehicle (PHEV) and Fuel Cell Electric Vehicle (FCEV)	Total electrical storage capacity of the EV's battery in kilowatt-hours (kWh), reflecting the maximum energy the battery can store and is essential for understanding the vehicle's power capabilities and potential range. For unknown capacity, a battery capacity of small, medium and large mentioned from the specific sourced were used	Percentage of the battery's capacity that was charged at the time of the experiment, a crucial factor in fire dynamics as it potentially affects the severity of a potential battery fire	Specific chemistry and construction of the battery cells used in the experiments, Lithium-ion Battery (LiB) if the cathode–anode were not mentioned specifically, Nickel Manganese Cobalt (NMC), or Lithium-ion manganese oxide (LMO) when mentioned specifically. Also, when known, the way cell was loaded were mentioned	Details about the state of the vehicle prior to ignition, specifically focusing on whether any doors or windows were open	Exact point where the fire started. It's important to note that some sources include the incipient stage – the early phase of the fire – in their heat release rate curves. This inclusion, or lack thereof, is clearly marked in a separate column for clarity	Additional fuel used to initiate the fire

Table 2 Information for EV fire experiments

ID	Vehicle Description/Model	Year manufactured	EV types	Battery capacity	Battery state-of-charge, %	Battery cell type	Condition	Ignition location	Ignition source	Incipient stage	Heat release rate evaluation method	References
EV1	Van	2019	BEV	40 kWh	80	Pouch, NMC	Not mentioned	Under battery pack	Propane burner (30 W)	NO	Oxygen consumption calorimetry	[17]
EV2	Small	2016	BEV	24 kWh	80	Prismatic, NMC	Not mentioned	Under battery pack	Propane burner (20 W)	NO	Oxygen consumption calorimetry	[17]
EV3	-	2014	BEV	Large	100	LiB	Windows closed	Under battery pack	Propane burner (2 MW)	NO	Oxygen consumption calorimetry	[18]
EV4	-	2013	BEV	Large	85	LiB	Windows closed	Under battery pack	Propane burner (2 MW)	NO	Oxygen consumption calorimetry	[18]
EV5	-	2013	BEV	Large	100	LiB	Windows closed	Under battery pack	Propane burner (2 MW)	NO	Oxygen consumption calorimetry	[18]
EV6	-	2013	PHEV	Small	85	LiB	Windows closed	Under battery pack	Propane burner (2 MW)	NO	Oxygen consumption calorimetry	[18]
EV7	-	2014	PHEV	Medium	100	LiB	Windows closed	Under battery pack	Propane burner (2 MW)	NO	Oxygen consumption calorimetry	[18]
EV8	-	-	BEV	16.5 kWh	-	LiB	Windows opened	Left front seat	Propane burner	NO	Oxygen consumption calorimetry	[19]
EV9	-	-	BEV	23.5 kWh	-	LiB	Windows opened	Left front seat	Propane burner	YES	Oxygen consumption calorimetry	[19]
EV10	Nissan Leaf	2011	BEV	24 kWh	100	LiB	Windows closed	Left rear bumper	80g alcohol gel fuel	YES	Mass loss rate	[20]
EV11	Compact car	2020	BEV	80 kWh	-	NMC	Fire blanket applied after 500s	Battery thermal runaway triggered	Liquid NaCL injection	YES	Enthalpy of the mass flow upstream	[21, 22]
EV12	Utility van	2016	BEV	24 kWh	-	LMO	-	Below floor plate	Propane burner	NO	Enthalpy of the mass flow upstream	[21, 22]

Table 2 (continued)

ID	Vehicle Description/Model	Year manufactured	EV types	Battery capacity	Battery state-of-charge, %	Battery cell type	Condition	Ignition location	Ignition source	Incipient stage	Heat release rate evaluation method	References
EV13	Sport Utility Vehicle	2020	BEV	80 kWh	-	NMC	-	Battery thermal runaway triggered	Liquid NaCL injection	NO	Enthalpy of the mass flow upstream	[21, 22]
EV14	Sport Utility Vehicle	2020	FCEV	1.56 kWh	20	LiB	25% windows opened	Around battery pack	50 ml n-heptane	NO	Oxygen consumption calorimetry	[12]
EV15	Sport Utility Vehicle	-	BEV	39 kWh	100	NMC	50% windows opened	Under car	Propane burner	NO	Oxygen consumption calorimetry	[12]
EV16	Sport Utility Vehicle	-	BEV	64 kWh	100	NMC	50% windows opened	Around battery pack	Heating sheet	NO	Oxygen consumption calorimetry	[12]

combustion. 'Enthalpy of mass flow rate' indicates that the energy released during the combustion process was calculated by assessing the enthalpy, or heat content, of the mass flow rate of gases upstream from the fire. This method involves measuring the changes in thermal energy of the gases as they move away from the fire source, providing a comprehensive view of the total energy output of the combustion. 'Species-based calorimetry' refers to methods where the heat release rate was calculated using the depletion of O_2, or the generation of CO_2 and/or CO. All of the methods mentioned above, while not without limitations, remain practical and effective for estimating the HRR of complex fire scenarios involving lithium-ion batteries. This method may overestimate HRR specifically for batteries due to biases in capturing the unique combustion characteristics of battery components [15, 16]. Nonetheless, it provides a comprehensive measure of heat release rate, total heat output and oxygen consumption across diverse material types, which is essential for assessing fire behaviour in applications like fires in car parks. In EV fire assessments, which involve a combination of batteries, plastics, metals, and other materials, oxygen-based calorimetry captures the integrated fire dynamics, including how the battery interacts with other components. Although it may not be ideal for isolated battery tests, its consistency and interpretability make it the most viable approach for probabilistic assessment applications, allowing reliable comparisons across complex fire vehicle scenarios. Next, key observations from each vehicle fire experiment, covering both EVs and ICE vehicles, are discussed. These observations were drawn from the relevant references, and where available, time markers for significant events during the experiments were also noted. However, not all references provided specific timing, so for some events, the time markers were estimated within a range based on available information. Table 4 presents the key observations and important time markers for all EV experiments, while Table 5 summarizes these details for the ICE vehicle experiments.

The discussion of the observations from the EV experiments focuses primarily on the involvement of batteries, as the powertrain is the key difference in combustible materials between EVs and ICE vehicles. Analysing the time markers of significant incidents revealed that, in 7 out of the 16 EV experiments, battery involvement occurred before the peak HRR was reached, while in 8 experiments, the batteries became involved only after the peak HRR. In one experiment, limited information was available regarding the timing of battery involvement.

The profiles for heat release rates derived from the experimental data are showcased in Fig. 1 and Fig. 2. These figures juxtapose the heat release rate curves from various experiments within each defined category on a unified axis, facilitating a direct comparison. This approach emphasises the validity of the classification system and highlights the variability present in the data. The determination of the peak heat release rate and the time to reach peak heat release rate are extracted from the profile curves if not mentioned clearly from the source. In this study, total heat released values are directly taken from explicit mentions in the source materials, avoiding calculations due to instances where experiments ended or data recording stopped prematurely, impacting the accuracy of Total Heat Released (THR) estimations.

Time averaging of the heat release rate curves was not applied in this study. To ensure consistency in timing, the incipient stage of the fire was excluded, and time was standardised to begin from the onset of significant fire growth. For cases where suppression efforts occurred, only one experiment involved active suppression, and this suppression took place after the fire had reached its peak HRR. As this study focuses on the growth phase, this experiment was retained in the dataset to capture the relevant fire dynamics during the critical early stages.

Table 3 Information for ICE fire experiments

ID	Vehicle type	Vehicle make and model	Year manufactured	Fuel type	Fuel balance, Liter	Condition	Ignition location	Ignition source	Incipient stage	Heat release rate evaluation method	References
ICE1	Van	-	2011	Diesel	-	-	Liquid pool fire under the fuel tank	Diesel 500mm x 500mm pan	NO	Oxygen consumption calorimetry	[17]
ICE2	Sedan	-	2015	Petrol	FULL	-	Underneath centre of vehicle	Propane burner (2 MW)	NO	Oxygen consumption calorimetry	[18]
ICE3	Sedan	-	2013	Petrol	FULL	-	Underneath centre of vehicle	Propane burner (2 MW)	NO	Oxygen consumption calorimetry	[18]
ICE4	Medium	-	-	Diesel	FULL	-	Burner in left front seat	Propane burner, 6 kW	YES	Oxygen consumption calorimetry	[19]
ICE5	Medium	-	-	Diesel	FULL	-	Burner in left front seat	Propane burner, 6 kW	YES	Oxygen consumption calorimetry	[19]
ICE6	Small	HONDA FIT	2011	Petrol	10	Windows closed	Left rear splash guard	80g of alcohol gel fuel	YES	Mass loss rate	[20]
ICE7	Sport Utility Vehicle	-	2020	Diesel	-	-	Burning interior	-	NO	Enthalpy of the mass flow upstream	[21, 22]
ICE8	Minivan	-	2010	Diesel	50	-	Underneath floor plate	Gas burner	NO	Enthalpy of the mass flow upstream	[21, 22]
ICE9	Sport Utility Vehicle	HYUNDAI IX35	2020	Petrol	-	-	Combustible contents heated	Heptane pan fire	NO	Oxygen consumption calorimetry	[12]
ICE10	Minivan	-	-	Petrol	10	-	Engine compartment	Engine oil	NO	Oxygen consumption calorimetry	[23]
ICE11	Minivan	-	1990s	Petrol	10	Windows closed	Splash guard right rear wheel	-	NO	Mass loss rate	[24]

Table 3 (continued)

ID	Vehicle type	Vehicle make and model	Year manufactured	Fuel type	Fuel balance, Liter	Condition	Ignition location	Ignition source	Incipient stage	Heat release rate evaluation method	References
ICE12	Minivan	-	1990s	Petrol	10	Windows closed	Right front bumper	-	NO	Mass loss rate	[24]
ICE13	Minivan	-	1990s	Petrol	10	20cm windows opened	Centre of back row seat	-	NO	Mass loss rate	[24]
ICE14	Sedan	-	-	Petrol	0	-	Right tyre	Burner, 900kW	NO	Oxygen consumption calorimetry	[25]
ICE15	Sedan	HYUNDAI SONATA	1998	Petrol	0	Windows opened	Ignition passenger seat	-	NO	Oxygen consumption calorimetry	[26]
ICE16	Sedan	Renault Talisman	2020	Diesel	0	33% windows opened	Front side passenger	Heptane pan 12cm	NO	Oxygen consumption calorimetry	[13]
ICE17	Sedan	Renault Talisman	2020	Diesel	33	33% windows opened	Front side passenger	Heptane pan 12cm	NO	Oxygen consumption calorimetry	[13]

2.2 Design Fire Profiles Comparison

This work is expected to provide invaluable insights for fire engineers, particularly in designing safe car parks, by offering a detailed comparison of design fires in terms of HRR profiles in EV and ICE vehicle fires. As previously studied and assessed for its suitability to characterize design fire for a single passenger vehicle [2], these design fires are characterized by a combination of growth and decay curves, where the growth phase is described using a t-squared function;

$$\dot{Q}(t) = \alpha_{peak} t^2 \left(t \leq t_{max}\right) \tag{1}$$

In Eq. 1, $\dot{Q}(t)$ represents the heat release rate, expressed as a function of time, where *t,* denotes the duration from ignition until the peak heat release rate is reached, and α, peak symbolizes the coefficient of fire growth. This approach presupposes a certain fire geometry, illustrating a time-squared proportional relationship for fires that ignite and spread radially. Such a model incorporates variables including the rate of flame spread, the rate of mass loss, and the combustion heat value [27]. Incorporating the decay phase of the fire, the analysis extends to utilize an exponential decay method, but now characterizing the reduction in the heat release rate post-peak. This exponential decay follows a specific equation that mirrors the gradual diminishment of the fire's intensity over time. The exponential decay is such that;

$$\dot{Q}\,(t) = \dot{Q}_{\max} e^{\beta_{\exp}(t - t_{\max})} \;\; (t \geq t_{\max}) \tag{2}$$

By combining the growth method with this exponential decay approach, a complete design fire curve emerges, applicable to passenger vehicles as demonstrated in prior research [2]. Building upon the established methodologies, the design fires EVs and ICE vehicles can now be constructed, utilizing the available data points from the distributions. Such detailed modelling paves the way for a thorough comparison between the fire dynamics of EVs and ICE vehicles, with a particular emphasis on the growth phase of the fire.

However, to construct the proposed design fire, a method is required to capture the dynamics of the HRR over time from the HRR profiles of EV and ICE vehicles, representing both the fire's development and decay phases. The first step involves examining the collected HRR profiles to assess their suitability for fitting. Each profile will be fitted individually, beginning with the t-squared fire growth model to represent the initial increase in HRR as the fire develops. This will be followed by applying the exponential decay model to describe the reduction in HRR as the combustion process slows.

2.2.1 Fire Growth and Decay Phase Fitting Methodology

For the growth phase, the HRR was modelled using a t-squared function, which takes the form of a quadratic equation, as denoted by Eq. (1) where q represents the HRR, t is time, and α is the growth coefficient. This model reflects the typical acceleration in energy release during the initial stages of combustion, as fire develops and consumes fuel more rapidly. The t-squared function provides a detailed fit across each time interval, capturing the incremental increases in HRR as the fire grows. The parameter α was determined by fitting this t-squared function to the observed HRR data over time, which allowed for an

Table 4 Key observations for all EV experiments

ID	Key observations	Time markers estimation (min)	References
EV1	- External fire ignition - Continuous and intense gas release from underneath - Gas release gone	- 5 min (External fire ignition) - 24–27 min (Gas release – battery compromise) - 30 min 30 s (Gas gone)	[17]
EV2	- External fire ignition - Battery venting and popping (most intense) - Gas release almost gone	- 5 min (External fire ignition) - 27–32 min (Venting and popping – battery compromise) - 44–47 min (Gas gone)	[17]
EV3	- Battery data loss at 5 min - Similar HRR to ICEV between 5–10 min - Battery involvement delayed until 10 min - Higher state of charge affected time	- 5 min (Plastic cover burned) - 7 min (Voltage drop, battery compromise) - 14–15 min (Battery ignites)	[18]
EV4	- Plastic cover burned within 5 min - Higher HRR in the first 5 min - Voltage drop and battery compromise - Battery fully involved by 15 min	- 5 min (Data loss) - 5–10 min (Fire growth due to source) - 10 min (Battery fully involved)	[18]
EV5	- Peak HRR at 10 min, peak heat flux before 10 min - Battery involvement did not significantly contribute to HRR and heat flux levels - Rear battery compromised at 11 min, voltage dropped to 0 V - Sudden spikes and dips in thermocouple readings after 11 min, likely due to electrical interference - Front battery voltage dropped to 0 V at 16 min - Visible pops, flashes, and flares were observed near 12 min and just before 20 min	- 10 min (Peak HRR) - Before 10 min (Peak heat flux) - 11 min (Rear battery compromised) - 11–16 min (Spikes and dips) - 12 min (Popping sounds and flashes) - 16 min (Front battery compromised) - Just before 20 min (Flashes near rear wheel)	[18]
EV6	- Temperature decreased gradually from 800°C to 600°C over the test - Highest levels of HRR occurred between 6 and 10 min - Secondary peak in HRR at 15 min - Battery involvement began at 5 min, contributing to increased temperature and spikes in heat flux - Voltage in individual battery cells decreased to 0 V between 6 and 9 min - Visible sparks and popping sounds from battery pack between 13 and 16 min, followed by flashes and flares - Bright flashes and flares observed between 19 and 27 min but did not contribute significantly to HRR - Gas tank involvement likely contributed to the high HRR between 6 and 10 min	- 5 min (Battery involvement begins) - 6–9 min (Battery cell voltage drop) - 6–10 min (Gas tank involvement) - 6–10 min (Peak HRR) - 15 min (Secondary HRR peak) - 13–16 min (Sparks, pops, flashes from battery) - 19–27 min (Flashes and flares)	[18]

Table 4 (continued)

ID	Key observations	Time markers estimation (min)	References
EV7	- Temperatures remained constant at around 800°C throughout the test - Two large spikes in HRR between 7 and 9 min, along with increases in heat flux and intense flames from the rear - Flames observed to extend past the exhaust hood at 7–9 min, but HRR readings may be underestimations due to damaged sensors - Gas tank release likely caused the HRR and heat flux spikes - Voltage readings dropped to 0 V at 6 min, indicating battery compromise - Battery burning contributed to high HRR levels, but the battery pack did not cause large spikes - HRR and heat flux remained stable after 10 min until gradually decreasing by the end of the test - Small spike in HRR and heat flux at 19 min, unclear if it was battery-related	- 6 min (Battery compromised, voltage drop) - 7–9 min (Large HRR and heat flux spikes) - 7–9 min (Flames and potential underestimation of HRR) - 7–9 min (Gas tank release) - 9–13 min (Battery contributed to high HRR) - After 10 min (Gradual decrease in HRR and heat flux) - 19 min (Small HRR and heat flux spike)	[18]
EV8	- Pouch cell configuration - Battery voltage at 400V - Temperature at battery reached 800°C - Gas venting and popping sounds between 12–15 min - Flames visible	- 5 min (External fire ignition) - 12 min (Battery compromised) - 15 min (HRR peak) - 12–20 min (Gas release duration)	[19]
EV9	- Prismatic cell configuration - Battery voltage at 350V - Temperature at battery reached 750°C - Gas venting and popping sounds between 10–12 min - Gas release and small flames visible	- 5 min (External fire ignition) - 10 min (Battery compromised) - 12 min (HRR peak) - 10–18 min (Gas release duration)	[19]
EV10	- Fire originated at the rear bumper and spread to the roof in 9 min - Rear tires and luggage compartment ignited - Rear window shattered at 20 min - Gas outburst from the battery at 37 min lasting 1 min - Front window shattered at 40 min, flames intensified - Battery voltage dropped to 0V at 50 min - Complete burnout by 120 min	- 9 min (Fire reaches roof) - 20 min (Rear window shatters) - 37 min (Gas outburst from battery) - 40 min (Front window shatters) - 50 min (Battery voltage drops) - 120 min (Vehicle burnout)	[20]

Table 4 (continued)

ID	Key observations	Time markers estimation (min)	References
EV11	- Maximum HRR: 7 MW - Energy content: 2893 MJ - Number of cells of the battery involved in the fire from the beginning	- 0—5 min (Battery ignition) - 8.5 min (Suppressed using fire blanket after fire fully developed)	[21, 22]
EV12	- Maximum HRR: 4.9 MW - Energy content: 3792 MJ - Fire development observed - Exact amount of fuel unknown	- 1—6 min (Fire developed quickly)	[21, 22]
EV13	- Maximum HRR: 8.9 MW (secondary peak 6.3 MW) - Energy content: 4154 MJ - Battery ignition after 13 min - Fire extinguished after 17 min	- 13.7 min (Battery ignition) - 15 min (HRR peak) - 17.8 min (Fire extinguished)	[21, 22]

Table 4 (continued)

ID	Key observations	Time markers estimation (min)	References
EV14	Initial Stage: - Ignition of n-heptane in the trunk with the LIB pack - Smoke venting observed - Flame observed outside the trunk - Gas temperature in the trunk exceeded 300°C Growth Stage: - Fire stagnated at 600°C and regrew due to air inflow - Local temperature reached 700°C - Explosion in the trunk - Rear tyre ignited - Side windows melted LIB Pack and Tyre Ignition: - Rear bumper failed - Rear tyre ignited - LIB cells ignited - Temperatures exceeded 800°C Fully Developed and Decay Stage: - Gas temperatures remained around 1,000°C - Front tyres ignited - Front bumper failed - High heat flux observed - Small explosions intermittently observed	- 26.8 min (Ignition) - 27.7 min (Onset of smoke venting) - 33.6 min (Initial flame observed in trunk) - 37.1 min (Rear window melted down) - 37.6 min (Flame observed in front seat) - 40.2 min (Explosion in trunk) - 40.7 min (Rear tyre ignited) - 41.2 min (Rear-side window melted down) - 41.8 min (Front window began melting) - 43.0 min (Rear bumper dropped down) - 44.5 min (Rear tyre ignited) - 47.5 min (Front airbag exploded) - 48.4 min (Rear airbag exploded) - 53.6 min (Front tyre ignited) - 54.9 min (Another front tyre ignited) - 59.5 min (Explosion around front tyre) - 61.1 min (Front bumper dropped down) - 63.7 min (Explosion around front tyre) - 142.6 min (Specimen burned out)	[12]

Table 4 (continued)

ID	Key observations	Time markers estimation (min)	References
EV15	- Ignition in the trunk, smoke venting observed, flames spread to the interior - temperatures recorded in the cabin and trunk, significant increase in HRR - Explosions around airbag and tyre areas, flames spread rapidly to external vehicle parts - Complete burnout after peak temperatures and heat flux affected surrounding areas	- 0.0 min (Burner switched on) - 2.5 min (Rear tyres ignited) - 5.2 min (Flame observed in trunk) - 5.6 min (Flame observed in cabin) - 6.7 min (Front tyres ignited) - 6.8 min (Flame observed in motor room) - 10.8 min (Explosion observed at rear) - 11.1 min (Burner switched off) - 11.2 min (Explosion observed at rear) - 11.3 min (Explosion observed at front) - 22.5 min (Onset of thermal runaway) - 23.5 min (Explosion observed in cabin) - 25.3 min (Thermal runaway around rear) - 27.4 min (Thermal runaway at rear edge) - 27.9 min (Thermal runaway at rear) - 30.7 min (Thermal runaway at rear) - 39.0 min (End of thermal runaway)	[12]

Table 4 (continued)

ID	Key observations	Time markers estimation (min)	References
EV16	- Ignition observed, rapid flame spread within the vehicle - Temperatures reached over 1000°C in certain parts of the vehicle - Multiple explosions observed, including rear tyres and airbags - Fully developed fire, significant thermal impact on internal and external components	- 0.0 min (Onset of heating a LIB cell) - 16.5 min (Ignitor switched on) - 21.3 min (Onset of internal thermal runaway) - 22.0 min (First gas observation at pack) - 24.4 min (First flame observation at pack) - 25.2 min (Rear tyre ignition) - 26.6 min (Trunk combustion) - 27.6 min (Rear seat combustion) - 29.4 min (Front seat combustion) - 30.2 min (Rear bumper collapse) - 30.5 min (Front tyre ignition) - 30.7 min (Motor room combustion) - 34.0 min (Front bumper collapse) - 34.7 min (Electrical cut-off) - 39.9 min (Thermal runaway at rear-centre) - 46.2 min (Air-bag explosion) - 50.5 min (Thermal runaway at rear edge) - 53.5 min (Thermal runaway at rear centre) - 56.1 min (Thermal runaway at front centre) - 65.7 min (Thermal runaway at front edge) - 72.6 min (Thermal runaway at mid-edge)	[12]

Table 5 Key observations for all ICE vehicles experiments

ID	Key observations	Time markers estimation (min)	References
ICE1	- Rapid HRR growth after fuel tank rupture - Total heat released (THR) was 5.9 GJ - Mass loss of 252 kg, representing 19% of the vehicle mass - Effective heat of combustion was 23 MJ/kg due to high availability of combustible materials	- 5 min (External fire ignition) - 9.7 min (Fuel tank rupture) - 16 – 18 min (Diesel pool fire almost gone)	[17]
ICE2	- Temperature underneath reached approximately 800°C - HRR showed significant growth during the first 5 min - No significant spikes in temperature and heat flux after the initial rise - Fuel tank combustion contributed significantly to heat flux - Faster rise in heat flux compared to EVs due to gasoline involvement	- 0–5 min (Steady rise in temperature to 800°C.) - Around 6 min (Fuel involvement causing a sharp increase in HRR and heat flux.) - 10 min (Heat flux reaches a peak.) - After 10 min (No significant spikes or fluctuations, steady combustion of materials.)	[18]
ICE3	- Temperature underneath reached approximately 800°C with fluctuations - Temperature decreased around 7 min, corresponding to an increase in HRR and radiative heat flux - Gas tank release likely caused the temperature decrease - Heat flux increased as air mixed with fuel vapours - HRR peaked around 10 min due to gasoline contribution	- 7 min (Temperature decrease due to gas tank release, increasing HRR and heat flux.) - 10 min (HRR peaked due to gasoline contribution.) - 20 min (Steady burning with no significant increases in temperature or HRR.)	[18]
ICE4	- Fire development similar to EV8 - Maximal HRR: 4.8 MW - Effective heat of combustion: 6900 MJ - Heat of combustion: 36–36.5 MJ/kg	- Around 14 min (Peak HRR reached)	[19]
ICE5	- Maximal HRR: 6.1 MW - Effective heat of combustion: 10,000 MJ - Heat of combustion: 36–36.5 MJ/kg	- Around 18 min (Peak HRR reached)	[19]
ICE6	- Fire spread from rear bumper to tires and luggage compartment at 14 min - Gasoline vapour leakage from fuel filler cap contributed to flames and window shattering - Large flame observed in passenger compartment at 35 min - Total heat release for the vehicle was 4.3 GJ - Peak heat flux at 0.5 m from rear reached 23 kW/m^2 - Fire behaviour similar to EV10 in terms of flame propagation. (Same literature source for EV10)	- 14 min (Flame from rear bumper propagated along body surface.) - 35 min (Passenger compartment flame rapidly grew.) - 52 min (Large flame formed at front.) - 120 min (Fire burned out completely.)	[20]

Table 5 (continued)

ID	Key observations	Time markers estimation (min)	References
ICE7	- The vehicle was ignited by fire in the interior - HRR increased steadily with a peak of 4.9 MW - Diesel fuel intensified the fire	- 10 min (2 MW HRR observed.) - After 10 min (HRR increased to 3.5 MW over the next 5 min.)	[21, 22]
ICE8	- Vehicle's body contributed to fire as the tank was nearly empty - Peak HRR was lower compared to BV03, peaking at 2.3 MW	- 13 min (Peak HRR reached)	[21, 22]
ICE9	- Peak HRR: 7.66 MW observed during the test - Total heat released (THR): 8.08 GJ - Slower burning profile compared to BEVs. (EV15 and EV16) - Gradual increase in HRR over time	- 0 to 5 min (Rapid increase in HRR to around 3 MW.) - 5 to 15 min (Continued increase, with fluctuations.) - 17 min (Peak HRR at 7.66 MW.) - 30 to 50 min (Gradual decrease in HRR.)	[12]

Table 5 (continued)

ID	Key observations	Time markers estimation (min)	References
ICE10	- After ignition, the flame quickly spread from the engine compartment to the rear, with the front bumper and windows playing a crucial role in flame propagation - Visible smoke overflowed from the engine cover slit after ignition, followed by flames emerging from the radiator grille at around 11 min - At about 20 min, flames penetrated the passenger compartment, and the front windscreen was broken, leading to flames spreading along the outer roof of the vehicle - The burning intensity increased significantly after the rear and mid-windows shattered, and at 31 min, the flame reached the rear windshield, leading to full passenger compartment involvement - A cracked fuel pipe at 36 min resulted in oil leakage and flames around the tires, which increased the intensity of the fire - Two explosions from the transmission shaft, occurring about one minute apart, caused a rapid increase in flame height - At 42 min and 35 s, the fire's intensity weakened, allowing for manual extinguishment	- 0 min (Ignition at the cooling fan of the engine compartment) - 0.2 min (Visible smoke overflowed from the slit of the engine cover) - 9.9 min (Flames emerged from the radiator grille) - 10.9 min (Smoke entered the passenger compartment through the air conditioning grille) - 11.6 min (Front bumper burned out and fell off, leading to intense burning in the engine compartment) - 13.2 min (Right-front tyre burst) - 14.55 min (Left-front tyre burst) - 14.7 min (Front windscreen broke due to heat) - 21.1 min (Flames spread along the passenger compartment and the outer car roof) - 25.1 min (Left-rear window shattered) - 25.8 min (Left-mid window burst outward) - 25.9 min (Intense burning observed in the passenger compartment) - 26.4 min (Flames spread along the left body coating of the vehicle) - 26.6 min (Right-rear window shattered) - 27.5 min (The mouth of the filler pipe opened, and visible flames overflowed) - 28.3 min (Right-mid window fell off) - 29.3 min (Flames spread to the trunk door) - 31.9 min (Rear windscreen shattered, and the entire passenger compartment engulfed in flames) - 35.7 min (Left-rear tyre and oil tank caught fire intensely) - 36.5 min (Petrol leaked out, and flames emerged from the car's bottom) - 38.5 min (Right-rear tyre burst) - 39.4 min (The transmission shaft exploded with a loud sound) - 40.1 min (Another explosion from the transmission shaft, causing flame height to rise rapidly) - 42.6 min (Fire was suppressed, and the experiment concluded)	[23]

Table 5 (continued)

ID	Key observations	Time markers estimation (min)	References
ICE11	- The fire ignited at the splashguard of the right rear wheel and spread to the passenger compartment through a gap by 11 min - The right-rear tyre burst at 12 min, and flames shattered the rear window at 40 min and the windshield at 46 min - By 55 min, the fire fully engulfed the front compartment, and the whole car was consumed - The fire burned out completely at 100 min after ignition. |	- 0 min (Ignition at the splashguard of the right rear wheel) - 5 min (Splashguard was enveloped in flame) - 10.6 min (Flame spread to the roof height) - 11.3 min (Passenger compartment filled with smoke, flame disappeared) - 12 min (Right-rear tyre burst) - 39.6 min (Left-rear tyre was ignited) - 40.2 min (Rear window was broken) - 46.3 min (Windshield was broken) - 55 min (Flames spread into the front compartment, the whole car engulfed in flames) - 100 min (Fire burned out)	[24]
ICE12	- Ignition occurred at the right front bumper, with the right-front tyre igniting at 3.5 min and the left-front tyre bursting at 17.7 min - Flames penetrated the passenger compartment at 13 min, but the fire slowed due to oxygen shortage - At 43 min, the left-front window opened, allowing flames to engulf the passenger compartment - The fire spread to the rear compartment by 55 min and burned out by 90 min. |	- 0.0 min (Ignition at the right front bumper) - 3.5 min (Right-front tyre was ignited) - 8.6 min (Front tyre burst) - 13.5 min (Passenger compartment was smouldered) - 17.7 min (Left-front tyre burst) - 40 min (Fire died down) - 43.0 min (Left-front window felt open, flames emerged) - 55 min (Flames spread to the rear compartment, whole car engulfed in flames) - 90 min (Fire burned out)	[24]

Table 5 (continued)

ID	Key observations	Time markers estimation (min)	References
ICE13	- The fire began at the centre of the 3rd row seat, spread quickly, and filled the passenger compartment with smoke within 3 min - Flames emerged from the rear hatch around 7.5 min, breaking multiple windows between 17.5 and 22 min, causing the entire passenger compartment to become engulfed in flames - Gasoline was ignited at around 29.5 min, which significantly intensified the fire, spreading flames into the front nose - The fire fully consumed the front nose, tires, and windows by 40 min, and the fire burned out after 80 min	- 0 min (Ignition at the centre of the 3rd row seat) - 1 min (Flame grew up on the seat) - 2.25 min (Flame reached the ceiling) - 3 min (The passenger compartment was filled with smoke) - 7.5 min (Flame appeared from the gap in the rear hatch) - 17.5 min (Right-rear window was broken) - 18.5 min (Front nose was entirely enveloped in flame) - 19.5 min (Left-front tire burst) - 19.65 min (Left-front window was falling down) - 19.8 min (Left-mid window was broken) - 19.85 min (Windshield cracked) - 19.95–21.95 min (Horn sounded) - 22 min (Windshield was broken entirely) - 23.7 min (Right-rear window was falling off)- 25.2 min (Left-rear tire burst) - 29.5 min (Gasoline was ignited) - 29.5 min (Flame spread into the front nose) - 35.7 min (Right-front tire burst) - 40 min (Front nose was entirely enveloped in flame) - 47.5 min (Right-front tire burst) - 80 min (Fire burned out)	[24]
ICE14	- The fire ignited the right rear tyre at around 19.57 min, with flames spreading to other parts of the vehicle shortly after - Flames spouted from various windows, including the rear and front, with significant heat release reaching over 3,215 kW by 44 min, indicating a flashover - By 53 min, the left front part of the vehicle started burning intensively, marking the final stage of the fire development	- 19.6 min (Right rear tyre ignited) - 20 min (Facade chamber heating finished) - 33.4 min (Flame spouted from right rear window) - 37.2 min (Flame spouted from rear window) - 41.6 min (Flame spouted from almost entire front window) - 53 min (Left front lighting started intensive burning)	[25]

Table 5 (continued)

ID	Key observations	Time markers estimation (min)	References
ICE15	- The fire started in the passenger seat and spread to the driver and rear seats within 5 min - By 7 min, the fire had reached the fuel tank and later spread to the engine room and bumpers - After reaching its peak intensity, the fire gradually diminished and extinguished between 25 to 60 min	- 0 min (Ignition in passenger seat) - 2.5 min (Fire active in passenger seat) - 5 min (Fire spreads to driver and rear seats almost simultaneously) - 7 min (Fire spreads to fuel tank) - 16.7 min (Fire spreads to engine room) - 20 min (Fire spreads to bumpers) - 25–60 min (Fire goes out)	[26]
ICE16	- Windshield broke at 4 min, with flames spreading into the passenger compartment by 8 min - All windows were broken by 11 min, accelerating the fire's spread to both the front and rear sections - Fire spread toward the front wheel arches at 10 min and engulfed the front by 20 min - By 22–23 min, the fire penetrated the trunk compartment, leading to full combustion of the rear	- 4 min (Windshield partially broke) - 7 min (Windshield broke completely) - 8 min (Fire spread to rear passenger compartment, flames exiting through left rear window) - 9 min (Right rear window broke) - 11 min (Rear window broke) - 12 min (Front windows broke) - 10 min (Flames appeared at front wheel arch) - 13 min (Fire spread to right front fender) - 17 min (Fire spread to left rear tire) - 20 min (Full fire development in the front) - 22 min (Flames penetrated trunk compartment) - 23 min (Full combustion of the rear)	[13]

Table 5 (continued)

ID	Key observations	Time markers estimation (min)	References
ICE17	- Small flames appeared in the right front window at 9 min, with the windshield breaking by 11 min - Rear windows broke by 16 min, with an airbag explosion at 13 min - Diesel fuel tank was pierced at 31 min, causing further flames and melting of the bumper - By 33 min, the entire vehicle was fully engulfed in flames, with intense fire development in both the front and rear sections	- 9 min (Small flames appeared in right front window seal) - 10 min (Small flames appeared in rear window) - 11 min (Windshield broke completely) - 16 min (Front windows broke) - 16 min (Rear windows broke) - 31 min (Rear window pierced) - 13 min (Airbag explosion, spread to side-view mirrors) - 17 min (Fire spread to front bumper) - 28 min (Full fire development in front, bumper melted) - 24 min (Fire spread to left rear tires) - 31 min (Diesel tank pierced, bumper fell) - 33 min (Full fire development in the rear)	[13]

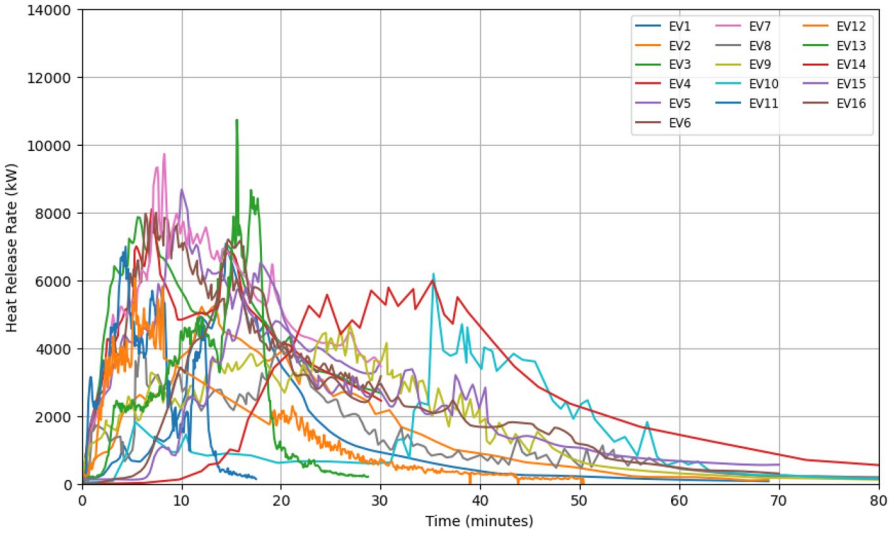

Fig. 1 Heat release rate profiles for EV fire experiments

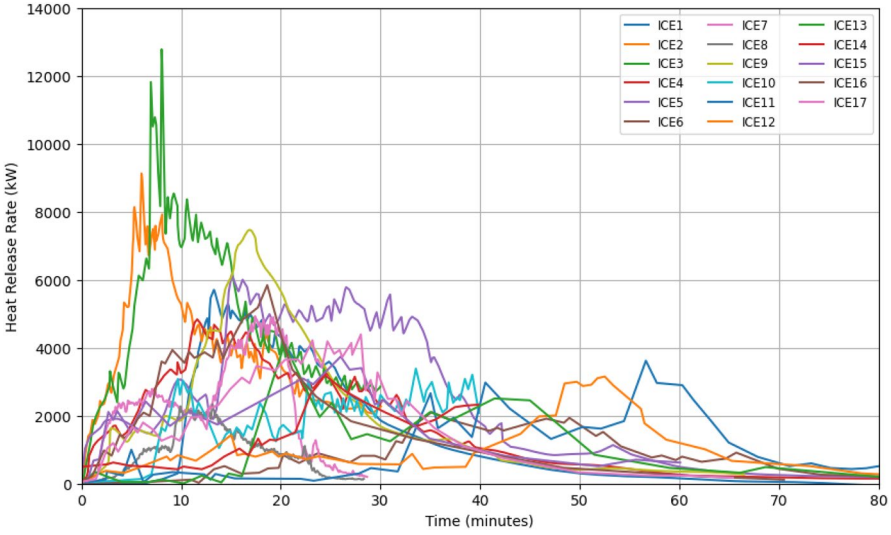

Fig. 2 Heat release rate profiles for ICE fire experiments

in-depth examination of the growth dynamics and yielded a specific value for the growth coefficient.

The growth phase fitting process concludes when it reaches the peak heat release rate (PHRR). To simplify identifying this peak, the approach intentionally disregards any lower peaks or periods of steady heat release. This focus on the highest peak provides a clearer understanding of the maximum potential fire intensity and growth rate for both EVs and

ICE vehicles. By emphasizing the highest peak, the methodology aims to deliver a more refined assessment of fire hazard, highlighting the critical role of growth in fire dynamics [2].

For the decay phase, the HRR was modelled with an exponential decay function, as denoted by Eq. (2), where Q_{max} is the PHRR, β is the decay constant, and t_{max} represents the time at which the HRR reaches its peak. The exponential decay model assumes that the HRR declines proportionally to its current value, reflecting the gradual reduction in combustion intensity as fuel is consumed. To facilitate parameter estimation, a logarithmic transformation of the model was performed, resulting in a linear form;

$$lnq = lnQ_{max} + \beta(t - t_{max}) \tag{3}$$

This transformation enabled the straightforward calculation of β and the conversion of the intercept, $ln(Q_{max})$, back to Q_{max} via exponentiation.

It is hypothesized that the quadratic fitting method will effectively capture the HRR growth profile, given its ability to incorporate detailed variations across each time step. This model's precision is expected to provide an accurate representation of the early combustion dynamics, in contrast to simplified approaches that might overlook the nuances of HRR progression over time. The exponential decay model is similarly anticipated to accurately reflect the decline phase, given its alignment with typical combustion behaviour where energy release decreases as fuel availability diminishes.

2.3 Experimental Data Analysis

This section focuses on transforming the collected experimental data into a meaningful resource that engineers can use to make informed decisions regarding appropriate design fires. The aim is to perform a statistical analysis of the collated data from previous section, with particular attention to identifying trends in the growth phase of vehicle fires. Given that the primary difference between EVs and ICE vehicles lies in their energy storage systems, analysing the growth phase is crucial. For EVs, batteries as energy storage can lead to rapid thermal runaway, potentially presenting unique fire dynamics compared to ICE vehicles.

Before conducting statistical analysis, however, it is necessary to make engineering decisions to determine the suitability of each dataset for inclusion. While this section will offer recommendations on dataset relevance, ultimately, engineers must decide which data are most applicable to their specific use cases. Therefore, the section will present all findings, allowing users to select the information that best aligns with their requirements while benefiting from the insights and trends identified here.

2.4 Filtering Experimental Data for Statistical Analysis

Based on a dataset of 16 EV and 17 ICE experiments gathered from the literature (as detailed in Tables 1, 2, 3, and 4), this subsection outlines the process of filtering experimental data for statistical analysis. The initial step involves reviewing each dataset to identify any prominent issues with the experimental setup that could introduce bias.

During this review, several tests were identified where the HRR of the ignition source reached or exceeded 2 MW, which could skew the analysis. These tests, with fires starting at such a large scale, do not accurately represent early-stage fire growth. Including these

data points could bias the statistical analysis, as the accelerated growth phase in these cases would misrepresent typical fire development. Consequently, tests EV3, EV4, EV5, EV6, EV7, ICE2, and ICE3 were excluded from the analysis.

Additionally, test EV14, involving a fuel cell electric vehicle (FCEV) with a small battery, was removed. Since the study focuses on the impact of different energy storage systems within vehicles, the inclusion of a fuel cell EV, which does not rely solely on battery energy storage, would not be relevant to the primary research objective. Thus, EV14 was excluded to maintain consistency in comparing EV and ICE vehicles based on battery involvement.

2.5 Data Analysis

This subsection presents the approach for analysing key metrics to draw meaningful insights on the fire characteristics of EV and ICE vehicles, supporting the development of representative design fire scenarios. The analysis centres on several important parameters, including Peak Heat Release Rate (PHRR), Time to Peak Heat Release Rate (TPHRR), and THR. These metrics provide valuable information about fire intensity, growth and decay rate, and overall energy output during combustion. Here, "peak" refers to the highest heat release rate observed, representing the maximum fire intensity reached during each experiment.

The primary focus of the data analysis is on calculating the fire growth coefficient, particularly within the growth phase of vehicle fires. This phase is essential for understanding potential hazards, as faster fire growth poses a greater threat due to rapid escalation in fire intensity. By comparing EV and ICE vehicles, the analysis aims to reveal whether EV fires, potentially influenced by battery involvement, exhibit a faster or different growth pattern than ICE vehicle fires.

Table 6 and Table 7 provide details on the PHRR, TPHRR, THR, growth and decay coefficients for both EVs and ICE vehicles. The growth and decay coefficients for both EVs and ICE vehicles were obtained using the fitting method explained in the Sect. 2.2.1. The data analysis only includes datasets that meet the filtering criteria explained in the previous subsection, ensuring a focused and reliable analysis. However, to provide comprehensive access to all collated data, Appendix 1 includes the full dataset, encompassing all vehicle experiments gathered.

Table 8 and Table 9 present comprehensive statistical analyses of the PHRR, TPHRR, THR, and growth coefficient for EV and ICE vehicles, respectively. These tables include the mode, median, mean, standard deviation, as well as the minimum and maximum readings for each variable. The statistical calculations derive from a filtrated dataset comprising 10 experiments for EVs and 15 for ICE vehicles. Notably, the mode is calculated under the assumption that the variables are discrete, an approach that facilitates understanding of the most frequent occurrence within the dataset.

The inclusion of mode, median, mean, and standard deviation is pivotal in statistical analysis, as each measure provides unique insights into the distribution of data. The mean offers a central value, while the median provides a midpoint that divides the dataset, helping to understand data skewness. The mode reveals the most common value, offering insights into the dataset's concentration. Standard deviation measures the dispersion around the mean, indicating the variability within the dataset. Collectively, these metrics allow for a nuanced interpretation of the data, aiding in

the identification of patterns, variability, and central tendencies within the statistical distribution.

It is crucial to acknowledge the inherently mathematical nature of these statistical calculations. The authors recognize that fire dynamics encompass a range of complex behaviours and interactions far beyond what can be directly captured through these statistics alone. However, the influence of probabilistic analysis in this context is significantly enhanced by the volume of available data. Although probabilistic methods might not yield exact predictions, they are instrumental in providing a general sense of the potential fire behaviour. By leveraging a substantial dataset, probabilistic analysis offers valuable insights into the characteristics of fire scenarios in terms of fire severity in the form of heat release rates, even amidst the inherent uncertainties and complexities of fire dynamics.

One important consideration is that, for the ICE vehicle experiments, data on the total energy released were limited, with only four data points available. As a result, the statistical analysis for this parameter may not be sufficiently extensive for broader application, and users of this analysis should take this limitation into account.

A nuanced interpretation of these findings is required, especially when considering the role of battery involvement in EV fires. When the battery does not contribute to the initial HRR, EV and ICE vehicles exhibit comparable fire characteristics due to similarities in materials used, such as interior fabrics and plastics. However, once the battery becomes involved, the fire dynamics of EVs shift considerably, with a tendency for more rapid-fire growth and higher peak intensities. This distinction highlights the importance of considering battery involvement in any fire scenario analysis, as it significantly affects the overall fire behaviour. Therefore, while general patterns between EVs and ICE vehicles are observable, the presence and timing of battery engagement in EVs are crucial variables that impact fire intensity and duration, underscoring the complexity and variability inherent in fire dynamics across vehicle types.

Table 6 Information of important characteristics for EVs fire experiments

Experiment ID	Peak heat release rate, $\dot{Q}_{max}$ (kW)	Time to reach peak heat release rate, t_{max} (min)	Total energy released (MJ)	Growth coefficient, α_{peak} (kW-min^{-2})	Decay coefficient, β (min^{-1})
EV1	6989	16.1	5200	29.8	– 0.08
EV2	5203	13.0	6700	25.5	– 0.07
EV8	4235	23.9	6314	4.1	– 0.05
EV9	4715	27.3	8540	3.4	– 0.07
EV10	6189	40.9	6400	1.3	– 0.07
EV11	6990	4.4	2800	295.9	– 0.28
EV12	6060	5.3	N/A	152.1	– 0.09
EV13	10,730	15.6	4454	22.4	– 0.31
EV15	6503	17.9	8450	21.3	– 0.05
EV16	7199	14.7	9030	33.3	– 0.05

Table 7 Information of important characteristics for ICE vehicles fire experiments

Experiment ID	Peak heat release rate, $\dot{Q}_{max}$ (kW)	Time to reach peak heat release rate, t_{max} (min)	Total energy released (MJ)	Growth coefficient, α_{peak} (kW-min^{-2})	Decay coefficient, β (min^{-1})
ICE1	5707	13.29	5900	36.5	– 0.08
ICE4	4800	15.09	N/A	26.4	– 0.06
ICE5	6100	18.28	N/A	12.7	– 0.06
ICE6	2107	23.38	N/A	1.3	– 0.05
ICE7	4930	17.50	3792	9.6	– 0.33
ICE8	2300	12.83	1540	14.1	– 0.20
ICE9	7660	20.34	8080	24.2	– 0.07
ICE10	3388	27.50	N/A	1.0	– 0.01
ICE11	3620	62.01	N/A	0.8	– 0.07
ICE12	3155	52.50	N/A	0.8	– 0.06
ICE13	4103	20.36	N/A	6.8	– 0.05
ICE14	3193	24.45	N/A	3.8	– 0.02
ICE15	3743	25.67	N/A	3.3	– 0.06
ICE16	5845	18.64	N/A	14.0	– 0.07
ICE17	4396	28.04	N/A	4.4	– 0.08

2.6 Distribution Fitting

The process known as distribution fitting is pivotal for accurately capturing the diverse behaviours of fire within a dataset. It involves selecting a statistical distribution that best represents the span of data relevant to different fire behaviours, particularly critical when analysing fire severity characteristics across the varied landscape of EVs and ICE vehicles. This study utilizes the JASP software, which is a free, open-source statistics software developed by the University of Amsterdam that offers both standard and advanced statistical techniques with a user-friendly drag-and-drop interface and real-time results display [28, 29]. The software offers three methodologies for determining the best-fit distributions

Table 8 The statistical distribution for EV fire experiments

Statistical attributes	Peak heat release rate, $\dot{Q}_{max}$ (kW)	Time to reach peak heat release rate, t_{max} (min)	Total energy released (MJ)	Growth coefficient, α_{peak} (kW-min^{-2})	Decay coefficient, β (min^{-1})
Mode	4234	4.4	2.8	1.4	-0.03
Median	6346	15.8	6.4	23.9	-0.01
Mean	6481	17.9	6.4	58.9	-0.01
Standard deviation	1799	10.7	2.1	94.1	0.09
Minimum	4234	4.4	2.8	1.4	-0.03
Maximum	10,730	40.9	9.0	296.0	0.00*

*Value too small

Table 9 The statistical distribution for ICE vehicle fire experiments

Statistical attributes	Peak heat release rate, $\dot{Q}_{max}$ (kW)	Time to reach peak heat release rate, t_{max} (min)	Total energy released (MJ)	Growth coefficient, α_{peak} (kW-min^{-2})	Decay coefficient, β (min^{-1})
Mode	2107	12.8	1.5	0.8	− 0.01
Median	4103	20.4	4.9	6.8	− 0.01
Mean	4336	25.3	4.8	10.6	− 0.01
Standard deviation	1524	13.9	2.8	10.9	0.08
Minimum	2107	12.8	1.5	0.8	− 0.03
Maximum	7660	62.0	8.1	36.5	0.00*

*Value too small

for fire severity characteristics: the Kolmogorov–Smirnov, Cramer-von Mises, and Anderson–Darling methods. Among these, the Kolmogorov–Smirnov method is selected due to its emphasis on the central part of the distribution, where most outcomes are concentrated, rather than focusing on the distribution's tails.

To conduct this fitting, several distributions are considered, including Gamma, Weibull, Exponential, Lognormal, and Normal, all with the lower bound set to zero to reflect the data's nature accurately. The selection process not only involves evaluating the fitting statistics—where a lower value indicates a more accurate fit—but also considers the frequency with which distribution shapes are used and their availability in other software for subsequent research.

The results of this analytical approach, showcasing the ranked order distributions PHRR, TPHRR and growth coefficient are meticulously compiled in Table 10 and Table 11. It is important to note that the analysis prioritizes these specific metrics as they are necessary in developing design fire scenarios, while the data for THR is currently not considered pivotal for this purpose. Additionally, a significant portion of the tests compiled lacks comprehensive information on THR, underlining our focused approach. For the decay coefficients, distribution fitting was not conducted, as both datasets consistently produced a fixed value of -0.01. Therefore, this value was established as the fixed decay coefficient. Accompanying these tables are the fitting statistics, providing a transparent and comprehensive view of how well each distribution fits the data, thereby maintaining the original intent of illustrating the methodological rigor applied in analysing fire severity characteristics within EV and ICE vehicle classifications.

In this statistical analysis, the distribution shape was chosen based on the lowest distribution fit value obtained for each dataset. For instance, when analysing the PHRR for both EV and ICE datasets, the Log Normal distribution provided the lowest distribution fit value for each. To streamline future distribution shape selections for PHRR data, the Log Normal distribution was therefore selected as a standard for this metric, given its consistent fit across both datasets.

However, determining the appropriate distribution shapes for TPHRR and growth coefficient was less straightforward, as the lowest distribution fit values did not correspond to a single distribution type for these parameters. For TPHRR the Gamma distribution was selected, as it consistently demonstrated low fit values across both EV and ICE datasets.

Table 10 The distribution fit ranking order for selected characteristics from EV fire experiments data

Rank	Peak heat release rate, $\dot{Q}_{max}$		Time to reach peak heat release rate, t_{max}		Growth coefficient, α_{peak}	
	Distribution shape	Value	Distribution shape	Value	Distribution shape	Value
1	*Log Normal*	*0.189*	Weibull	0.156	Log Normal	0.216
2	Gamma	0.205	*Gamma*	*0.176*	*Weibull*	*0.236*
3	Weibull	0.258	Normal	0.199	Gamma	0.275
4	Normal	0.691	Log Normal	0.215	Exponential	0.368
5	-	-	Exponential	0.315	Normal	0.413

Table 11 The distribution fit ranking order for selected characteristics from ICE vehicles fire experiments data

Rank	Peak heat release rate, $\dot{Q}_{max}$		Time to reach peak heat release rate, t_{max}		Growth coefficient, α_{peak}	
	Distribution shape	Value	Distribution shape	Value	Distribution shape	Value
1	*Log Normal*	*0.098*	Log Normal	0.182	*Weibull*	*0.137*
2	Gamma	0.099	*Gamma*	*0.219*	Gamma	0.138
3	Weibull	0.111	Weibull	0.254	Log Normal	0.148
4	Normal	0.123	Normal	0.287	Exponential	0.155
5	–	–	Exponential	0.398	Normal	0.190

For the growth coefficient, the Weibull distribution was chosen due to its consistently low fit values for both datasets.

The advantage of distribution fitting becomes more apparent when considering the variability and uncertainty inherent in fire behaviour. Summary statistics such as the mean, median, and mode provide central tendencies but fail to capture the full range of possible fire behaviours, particularly the likelihood of extreme events. In contrast, distribution fitting allows for the generation of percentile-based design fire inputs, enabling fire engineers to account for both typical and rare fire scenarios. This approach is particularly relevant in the context of EV fires, where variability in fire dynamics is influenced by factors such as battery involvement, ignition source, and vehicle configuration.

Distribution fitting also plays a critical role in addressing uncertainties associated with fire measurements. Even under controlled conditions, repeated fire tests of the same vehicle may yield slightly different HRR curves due to random variations in material properties, ignition points, or fire progression. By fitting distributions to the data, this analysis accommodates those natural fluctuations, allowing for more robust and adaptable fire safety assessments. Summary statistics alone may overlook these nuances, resulting in overly conservative or overly optimistic fire scenarios.

Furthermore, distribution fitting provides greater flexibility in tailoring design fires to specific risk tolerances. Fire engineers can select design fire inputs based on a desired percentile value, balancing conservatism and practicality in performance-based fire safety design. For instance, a design fire constructed using the 90th percentile value will capture more extreme fire behaviours, ensuring that infrastructure designs account for higher-risk

scenarios. This flexibility allows engineers to make informed decisions based on the specific safety objectives of their projects, rather than relying solely on average values that may not reflect the range of possible fire outcomes.

These distributional fits not only provide a structured way to comprehend the fire dynamics of EVs and ICE vehicles but also emphasise the differences in fire growth and intensity characteristics between the two vehicle types. By employing Log Normal for PHRR, Gamma for TPHRR, and Weibull for Growth coefficient, the analysis adeptly accommodates the skewed nature of these data, while the parameters μ and σ offer a detailed understanding of their distributions. The distribution parameters identified for EVs, and ICE vehicles are essential for creating probabilistic design fires for both types of vehicles for the use of simulation which are shown in Table 12.

2.7 Effect of Battery Sizes to Peak Heat Release Rate and Growth Coefficient for EV Experiments

This section examines the influence of battery size on the PHRR and growth coefficient in EVs, using data from the collated fire experiments. The objective is to determine whether there is a direct correlation between battery size and fire magnitude, as well as to understand how battery size affects fire growth dynamics. With larger batteries increasingly integrated into modern vehicles to support longer range and better performance, understanding this relationship is crucial.

For the EV fire experiments, a subset of 10 experiments—filtered from the total of 16—was analysed specifically to assess the impact of battery size on PHRR. The analysis was therefore limited to these 10 vehicles, for which battery sizes were documented. Figure 3 presents a log-scale graph illustrating the correlation between battery size and PHRR, revealing a logarithmic correlation with a coefficient of determination (R^2) of 0.73 based on a simple regression analysis. This significant correlation suggests a notable relationship, indicating that larger battery sizes are associated with higher PHRR values, which points to a quantifiable impact of battery capacity on fire intensity. However, given that this analysis was based on only 10 vehicles, it is important to acknowledge that conclusions drawn from this limited dataset may not fully capture the broader dynamics of EV fires.

The correlation between battery size and PHRR in EV fires has also been explored in recent studies, with Sun et al. [6] highlighting a similar relationship. While the current study found a logarithmic correlation, Sun et al. [6] established a power-law relationship and based on a larger dataset with various battery types and configurations, Sun et al.'s findings affirm the importance of battery size in influencing fire severity but also emphasize the roles of battery arrangement, cooling conditions, and air supply in fire behaviour. In contrast, the current study, with a smaller dataset, points to the need for further data to refine the observed correlation and suggests that battery size is just one of multiple factors affecting fire risks in EVs.

Further insight into the relationship between battery size and PHRR comes from Willstrand et al. [17], whose study focused on isolated battery fire tests rather than full EV fires. Although Willstrand et al. observed a positive correlation between battery energy capacity and PHRR, their findings were limited to individual battery cells and packs, without the additional materials and components present in an EV. This distinction is crucial, as EV fires involve other combustibles such as plastics, metals, and interior materials that can significantly affect fire dynamics. Despite these differences, Willstrand's findings align with the general trend observed in the current study, reinforcing the notion that battery size

Table 12 Distribution parameters for the selected characteristics of EVs and ICE vehicles fire experiments

Classification	Peak heat release rate, $\dot{Q}_{max}$		Time to reach peak heat release rate, t_{max}		Growth coefficient, α_{peak}	
	Log Normal		Gamma		Weibull	
	μ	σ	λ	κ	λ	κ
EVs	8.75	0.25	2.87	6.23	0.68	43.8
ICEs	0.83	0.35	4.93	5.15	0.94	10.34

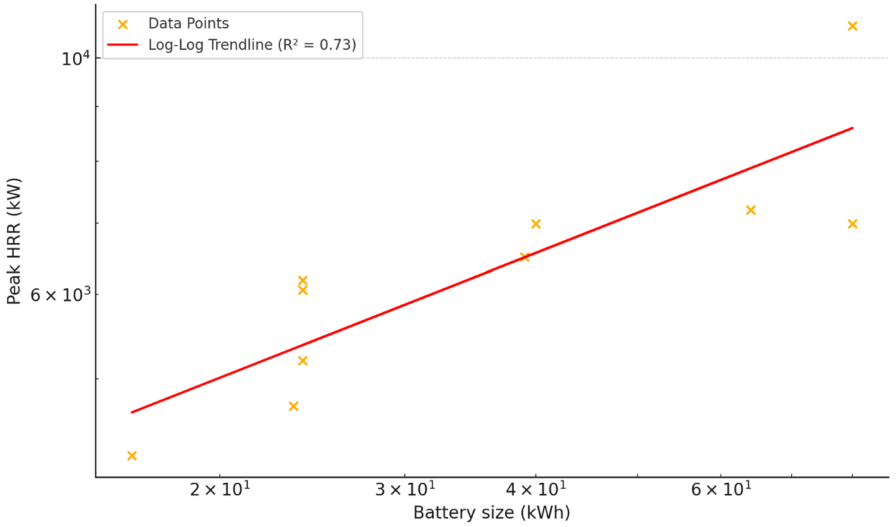

Fig. 3 The relationship between battery size and the peak heat release rate of EV fire experiments

correlates with fire intensity. However, the complexity of full-scale EV fires suggests that extrapolating from battery-only tests may not capture the complete fire behaviour in EV scenarios.

The investigation further extends to analysing the relationship between battery size and the corresponding growth coefficient across the same subset of 10 EV experiments, as shown in Fig. 4. This phase of the analysis aims to determine whether battery size has a measurable effect on the rate of fire growth—a critical factor in understanding fire dynamics and safety implications in EVs. Using a simple regression analysis with a logarithmic trend line, a coefficient of determination (R^2) of 0.31 was obtained. While this value indicates some correlation, it suggests that battery size does influence the rate of fire growth, albeit to a moderate extent.

In interpreting these results, it is essential to consider additional factors that may affect the growth coefficient, such as the location of ignition (interior or exterior), ignition power, timing of battery involvement, and the specific battery types and technologies used. Each of these factors can significantly influence fire dynamics—yet in real-world scenarios, they are often beyond control and inherently random. This analysis takes a broad, inclusive approach, acknowledging the variability and unpredictability of these elements. The goal is

to establish a foundational understanding that can accommodate this randomness. As more data becomes available, we anticipate that clearer trends will emerge, even amidst the variability of these uncontrolled factors, ultimately allowing for a more reliable prediction of fire growth in EVs.

Building on these initial findings, it is essential to approach the observed correlation between battery size and fire growth coefficient in EVs with caution. EVs are highly complex systems and cannot be considered as simple, homogenous objects where straightforward correlations might apply. They involve multiple dimensions, varying materials in both interior and exterior construction, and diverse battery placement configurations, all of which add to their complexity. Additionally, numerous other factors affect fire dynamics, including the ignition location and the types of materials inside the vehicle. For example, different ignition points can significantly alter fire behaviour and potentially impact fire magnitude.

2.8 Design Fire Profiles Comparison

One potential application of the analysed data is the construction of a design fire model that fire engineers can use to assess fire behaviour in various scenarios. In this section, an example design fire is developed based on the data presented in Table 6 and Table 7, utilizing the mean (average) values derived from the statistical distributions to create a representative fire scenario. The primary objective behind formulating these mean design fires for EVs and ICE vehicles is to facilitate a comparative visualization of the potential hazards associated with fires in these vehicle categories. This visual comparison is essential for understanding the distinct fire behaviour and risks presented by each type of vehicle during fire incidents. By constructing design fires for both EV and ICE vehicles, this model allows for a straightforward comparison.

It is important to highlight that the ICE vehicle data included in this analysis represents the most recent information gathered in the current study. Furthermore, to provide a comprehensive perspective on the evolution of vehicle fire hazards, a design fire model based on data collated in previous research, specifically for ICE vehicles up to the year 2013 as documented by Tohir et al. [9], has also been developed. This historical comparison allows the authors to juxtapose the design fire characteristics of ICE vehicles across different time frames (up to 2013 and 2014–2023) against those of EVs.

The comparative study of design fire profiles using the mean (average) distribution over time among EVs, ICE vehicles up to 2013, and ICE vehicles from 2014 to 2023 reveals distinct fire development behaviours across these vehicle categories as shown in Fig. 5. For EV), the design fire reaches its PHRR at approximately 19 min, while the ICE vehicles from 2014–2023 reach their PHRR around 20 min. Notably, the PHRR for EV fires is approximately 2000 kW higher than that of the ICE2014–2023 fires. Comparing fire growth is more meaningful when we consider the time required to reach a particular HRR. By choosing a common HRR target of 4000 kW, we observe that the EV design fire reaches this level at about 15 min, whereas the ICE2014–2023 design fire reaches it around 19 min. This difference indicates that EV fires grow slightly faster, and the 4-min lead time is critical. A quicker growth rate means that EV fires have a greater potential for rapid spread, increasing the urgency for effective suppression or containment. Looking at older ICE vehicles (pre-2013), the design fire reaches 4000 kW around 27 min, significantly slower than ICE2014–2023. This quicker escalation in newer ICE vehicles may reflect the

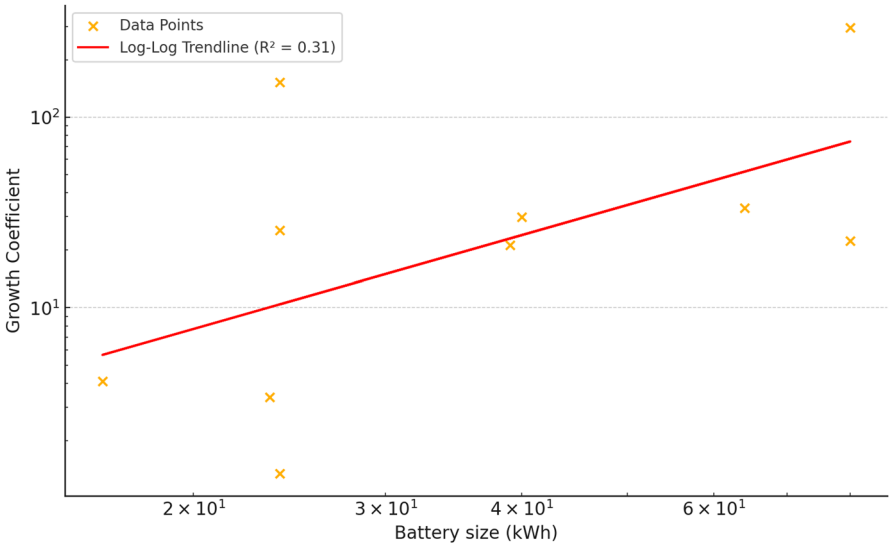

Fig. 4 The relationship between battery size and the growth coefficient of EV fire experiments

increased use of combustible materials, such as polymeric or plastic components, which accelerate the growth rate of fires [10, 27].

The faster growth dynamics observed in EV fires hold critical implications for fire engineering, as the quicker a peak HRR is reached, the more rapidly heat is radiated to combustibles in the vicinity, leading to a faster spread of fire. The data further reveal that EVs, on average, exhibit a peak HRR approximately 2000 kW higher than that of ICE vehicles. Such a significant difference in PHRR highlights the heightened risk of fire spread in scenarios involving EVs, particularly in environments like car parks. This suggests that fires involving EVs not only have the potential to grow larger but also to spread more quickly. Given that this analysis is based on a limited dataset, if these findings hold true, they will pose considerable challenges to existing fire safety strategies and necessitate a re-evaluation of response protocols to better address the unique risks presented by EVs.

Further analysis has been conducted to integrate the generated mean design fire curves, constructed using average HRR values, onto the family of HRR curves for EV and ICE vehicles, as shown in Fig. 6 and Fig. 7, respectively. This approach aims to illustrate how the mean design fire curves align within the broader set of observed HRR curves. Both plots indicate that the generated design fire curves follow a conservative and reasonable trajectory relative to the family of curves, supporting their relevance as representative fire scenarios. It is noted, however, that these design fires are based on average values. To provide a more conservative and practical option for fire safety applications, an 80th percentile design fire curve has now been included in Figs. 6 and 7. The 80th percentile curve represents a more extreme fire scenario compared to the mean design fire, aligning more closely with the approach typically taken by fire engineers when selecting conservative design fires. The use of probabilistic inputs—such as percentile values—could yield design fires that occupy different positions within the family of curves, potentially offering a more nuanced perspective on fire growth and severity by accommodating a range of HRR outcomes. The addition of the 80th percentile curve highlights how percentile-based design fires can better account for variability, providing fire engineers with flexibility to choose

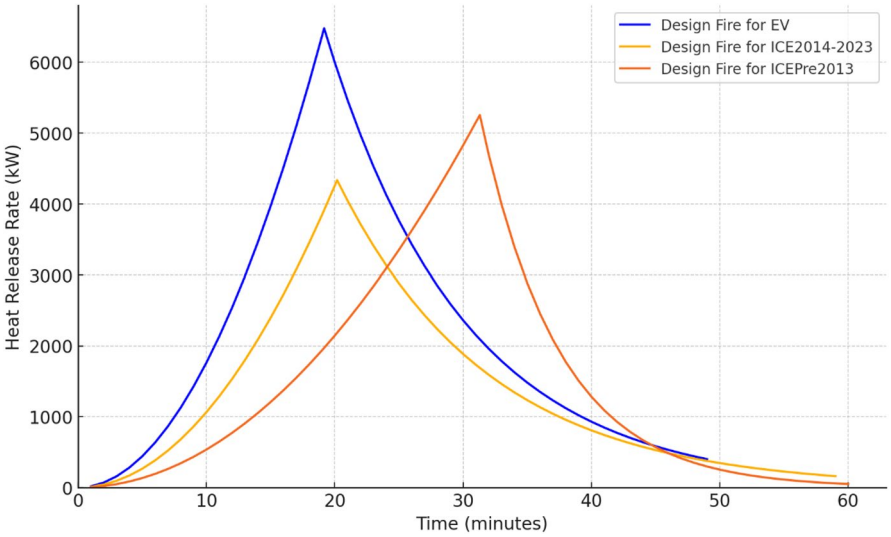

Fig. 5 Comparative design fire profile for EV and ICE vehicles using mean (average) distribution

design fires that reflect different levels of risk tolerance. This variability shows the importance of statistical analysis in performance-based fire safety design, where accurately representing the HRR data is essential for developing reliable design fire models [30].

In another analysis, Fig. 8 shows HRR curves for various passenger vehicle design fires, which are typically utilized by fire engineers when designing buildings involving vehicles, such as parking structures or tunnels. These design fires serve as critical input parameters for performance-based fire safety engineering, influencing decisions related to fire suppression systems, structural integrity, and ventilation. The figure juxtaposes the 80th percentile heat release rate curves for both EVs and ICEs against several commonly used reference design fires from literature, including Joyeux[31], the New Zealand Verification Method C/VM2[32], TNO[33] and Ingason's models[34]. The comparison aims to assess whether the existing reference design fires remain adequate in representing the fire hazards posed by modern vehicles. From the figure, it can be observed that the 80th percentile curve for ICE vehicles lies somewhere in the middle of the spectrum compared to the reference plots. It is neither overly conservative nor excessively lenient. This positioning is expected, given that the curve is derived from statistical distribution rather than worst-case assumptions. Using a distribution-based design fire ensures that the approach is data-driven and avoids overly conservative assumptions that could lead to unnecessary construction costs. Ultimately, fire engineers can decide on the level of conservatism required based on the data presented, balancing safety with economic considerations.

However, the 80th percentile curve for EVs appears to be among the most conservative curves shown in the plot. This raises a critical question: does this suggest that the existing reference design fires are no longer conservative enough for modern EV fire scenarios? This observation warrants further investigation. It could indicate that EVs may present higher fire risks compared to traditional vehicles, especially since existing reference plots, such as Ingason's from 2006, were developed before the widespread adoption of modern EV technology. Alternatively, it may reflect inherent differences in the fire dynamics of EVs, as battery fires can release energy suddenly, though this does not necessarily result in

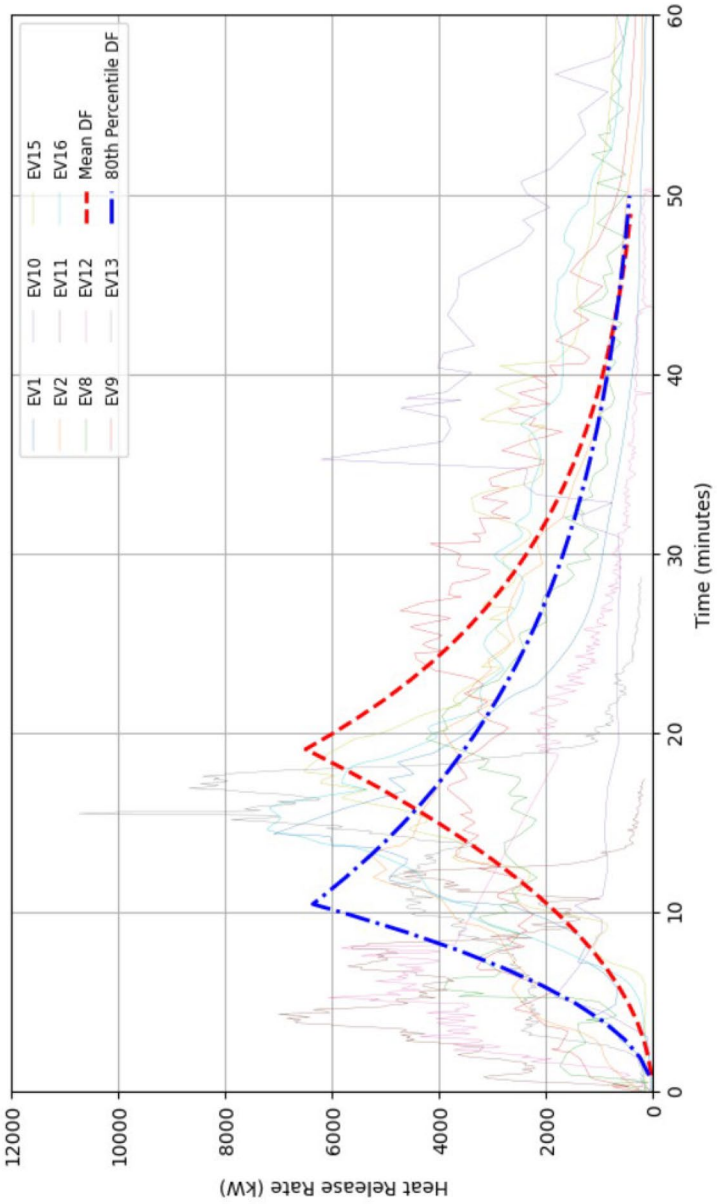

Fig. 6 Comparison of mean design fire against the HRR curves for all EV experiments

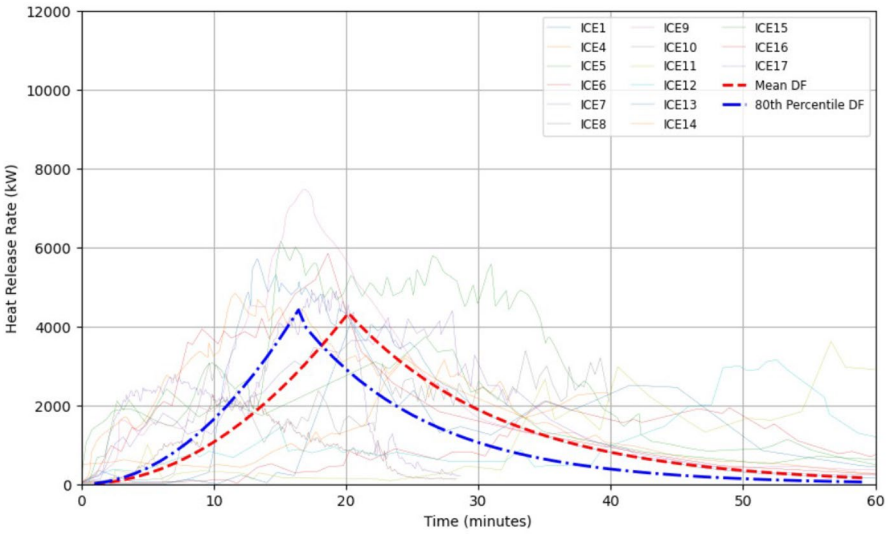

Fig. 7 Comparison of mean design fire against the HRR curves for all ICE experiments

larger or quicker fires compared to ICE scenarios. While the current reference plots appear sufficient for ICE vehicle scenarios, the EV design fire curve's positioning suggests that fire engineers may need to reconsider the conservatism of reference plots when accounting for EVs in building fire safety designs.

A key implication of reconsidering reference plots for modern fire scenarios, particularly those involving EVs, is the need to revisit how design fires are characterised in fire risk assessments. The design fire, typically represented by the HRR as a function of time, serves as a primary input for analyses ranging from simplified hand calculations to complex computational fluid dynamics (CFD) simulations. HRR data is generally derived from experimental methods, such as oxygen consumption calorimetry, to ensure accuracy in representing fire behaviour. Nevertheless, the inherent variability of fire dynamics means that repeated tests under identical conditions often yield HRR curves with minor discrepancies. This variability highlights the importance of using statistical methods to generate a representative reference curve that accommodates natural fluctuations in fire behaviour. By statistically analysing multiple datasets, a more robust and generalisable design fire curve can be developed, enhancing the reliability of performance-based designs in accommodating the unpredictable nature of real-world fire scenarios. This approach ensures that fire safety assessments are not only grounded in empirical data but also account for the uncertainties and complexities inherent in fire dynamics, thus supporting a more resilient and adaptable design framework.

2.9 Discussions and Concluding Remarks

In conclusion, this study provides a comprehensive analysis of heat release rate profiles between EVs and ICE vehicles, highlighting key differences in fire behaviour, particularly in terms of growth and peak heat release rates. Through detailed statistical

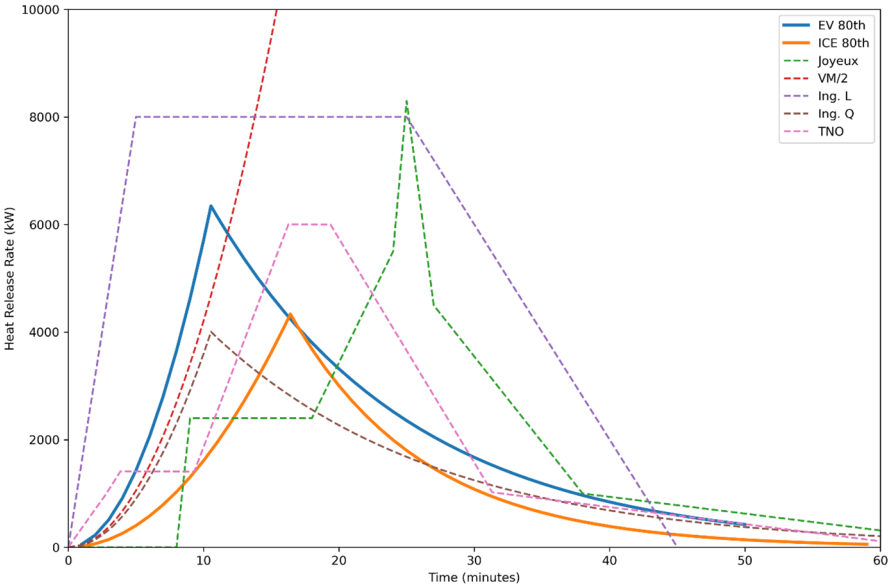

Fig. 8 Design fire curves for the 80th percentile of EV and ICE compared to reference design fires for passenger vehicles

analysis, this research demonstrates the influence of battery involvement in EV fires, with findings indicating that larger battery sizes correlate with higher peak heat release rates. The design fire models developed from this data offer valuable insights, equipping fire engineers with an alternative, probabilistic approach for simulating vehicle fire scenarios, beyond traditional deterministic methods for performance-based design. By incorporating probabilistic design fire inputs, this work broadens the toolkit for fire engineers, allowing for more informed and flexible decision-making in fire risk assessments and design.

This probabilistic approach differs from that of Hodges et al. [35], who established a model aimed at conservatively bounding design fires for passenger vehicles. Their model uses vehicle parameters such as battery energy capacity, curb weight, and gas tank capacity and was validated with full-scale fire test data to offer consistently conservative predictions of HRR and THR. This makes their model suitable for assessing fire hazards in a range of vehicle types, especially larger, high-energy-capacity vehicles. In contrast, the current study's probabilistic framework provides a flexible alternative, allowing fire engineers to simulate a range of potential scenarios that can be refined as more data becomes available. While Hodges et al. advocate for a bounding, deterministic model, this study's probabilistic design approach offers adaptability in assessing fire risks, particularly as vehicle technologies evolve.

As fire engineers work towards creating safer infrastructure and response measures for both vehicle types, this research provides essential guidance for designing targeted fire scenarios. The comparison between EV and ICE vehicles emphasises the need for continuous research and adaptation of fire safety standards to address the unique risks introduced by technological advancements. It is important to note, however, that this analysis is based on a limited dataset, and while informative, future studies should seek to expand the dataset

with more varied experimental results to further refine our understanding of vehicle fire dynamics.

Future research efforts should focus on incorporating diverse experimental data to capture a wider spectrum of vehicle fire behaviours, particularly as new EV models and configurations are introduced. This expanded dataset will better equip the fire safety community to anticipate and mitigate fire risks across different environments. This foundational work paves the way for improvements in performance-based design of infrastructure, enabling fire safety professionals to make more informed decisions that address the unique challenges posed by electric mobility and evolving vehicle fire risks.

Supplementary Information The online version contains supplementary material available at https://doi.org/10.1007/s10694-025-01711-3.

Acknowledgements This project has received funding from the European Union's Horizon Europe research and innovation programme under the Marie Skłodowska-Curie Actions (MSCA) grant agreement ID: 101064984.

Funding Open Access funding provided thanks to the CRUE-CSIC agreement with Springer Nature. This work was funded by HORIZON EUROPE Marie Sklodowska-Curie Actions, 101064984, Mohd Zahirasri Mohd Tohir

Declarations

Conflict of interests The authors declare that they have no conflict of interest.

Ethical Approval During the preparation of this work the author(s) used Open AI ChatGPT 4 in order to fix any grammatical errors in the text and for language clarity purposes.

Consent for Publication After using this tool/service, the author(s) reviewed and edited the content as needed and take(s) full responsibility for the content of the publication.

References

1. Brzezińska D, Bryant P (2021) Risk index method—a tool for building fire safety assessments. Applied Sciences (Switzerland). https://doi.org/10.3390/app11083566
2. Tohir MZM, Spearpoint M, Fleischmann C (2020) Probabilistic design fires for passenger vehicle scenarios. Fire Saf J. https://doi.org/10.1016/j.firesaf.2020.103039
3. Yung DT, Benichou N (2002) How design fires can be used in fire hazard analysis. Fire Technol. https://doi.org/10.1023/A:1019830015147
4. Mohd Tohir MZ, Martín-Gómez C (2023) Electric vehicle fire risk assessment framework using fault tree analysis. Open Research Europe. 3(178):178. https://doi.org/10.12688/openreseurope.16538.1
5. Sander L, Zehfuß J, Meyer P, Schaumann P (2021) Brandrisiko von E-Fahrzeugen und kraftstoffbetriebenen Fahrzeugen in offenen, oberirdischen Parkgaragen: Teil 1: Brandszenarien und Brandeinwirkungen. Stahlbau. https://doi.org/10.1002/stab.202100039
6. P. Sun, R. Bisschop, H. Niu, and X. Huang, *A Review of Battery Fires in Electric Vehicles*, vol. 56, no. 4. Springer US, 2020. https://doi.org/10.1007/s10694-019-00944-3.

7. A. Dorsz and M. Lewandowski, "Analysis of fire hazards associated with the operation of electric vehicles in enclosed structures," 2022. https://doi.org/10.3390/en15010011.
8. Tohir MZM, Spearpoint M (2014) Development of fire scenarios for car parking buildings using risk analysis. Fire Safety Science 11:944–957. https://doi.org/10.3801/IAFSS.FSS.11-944
9. Tohir MZM, Spearpoint M (2013) Distribution analysis of the fire severity characteristics of single passenger road vehicles using heat release rate data. Fire Sci Rev 2(1):5. https://doi.org/10.1186/2193-0414-2-5
10. J. Hynynen *et al.*, "Electric Vehicle Fire Safety in Enclosed Spaces," Sweden, 2023.
11. Boehmer HR, Klassen MS, Olenick SM (2021) Fire hazard analysis of modern vehicles in parking facilities. Fire Technol 57(5):2097–2127. https://doi.org/10.1007/s10694-021-01113-1
12. Kang S, Kwon M, Yoon Choi J, Choi S (2023) Full-scale fire testing of battery electric vehicles. Appl Energy. https://doi.org/10.1016/j.apenergy.2022.120497
13. O. Willstrand, J. Gehandler, and P. Andersson, *Proceedings from the Seventh International Conference on Fires in Vehicles*. RISE Sweden, 2023.
14. Biteau H et al (2008) Calculation methods for the heat release rate of materials of unknown composition. Fire Safety Science. https://doi.org/10.3801/IAFSS.FSS.9-1165
15. Fu Y, Lu S, Li K, Liu C, Cheng X, Zhang H (2015) An experimental study on burning behaviors of 18650 lithium ion batteries using a cone calorimeter. J Power Sources. https://doi.org/10.1016/j.jpowsour.2014.09.039
16. Zhang W et al (2015) Combustion calorimetry of carbonate electrolytes used in lithium ion batteries. J Fire Sci. https://doi.org/10.1177/0734904114550789
17. O. Willstrand, R. Bisschop, P. Blomqvist, A. Temple, and J. Anderson, "Toxic Gases from Fire in Electric Vehicles," 2020.
18. 2016 FIVE, "4th International conferenceon Fire in Vehicles - FIVE 2016 Conference, International," in *Fires in Vehicles - FIVE 2016 October 5–6, 2016*, 2016.
19. A. Lecocq, M. Bertana, B. Truchot, and G. Marlair, "Comparison of the Fire Consequences of an Electric Vehicle and an Internal Combustion Engine Vehicle .," in *International Conference on Fires in Vehicles*, 2012.
20. N. Watanabe *et al.*, "Comparison of fire behaviors of an electric-battery-powered vehicle and gasoline-powered vehicle in a real-scale fire test," *Second International Conference on Fires in Vehicles*, no. 2, 2012.
21. Sturm P et al (2023) Dataset of fire tests with lithium-ion battery electric vehicles in road tunnels. Data Brief. https://doi.org/10.1016/j.dib.2022.108839
22. Sturm P et al (2022) Fire tests with lithium-ion battery electric vehicles in road tunnels. Fire Saf J. https://doi.org/10.1016/j.firesaf.2022.103695
23. Hu Y, Zhou X, Cao J, Zhang L, Wu G, Yang L (2020) Interpretation of fire safety distances of a minivan passenger car by burning behaviors analysis. Fire Technol. https://doi.org/10.1007/s10694-019-00938-1
24. Okamoto K, Otake T, Miyamoto H, Honma M, Watanabe N (2013) Burning behavior of minivan passenger cars. Fire Saf J. https://doi.org/10.1016/j.firesaf.2013.09.010
25. Yoshioka H, Iwami T, Takeya S (2018) Experimental study on car fire with respect to urban fire spreading. Fire Science and Technology. https://doi.org/10.3210/fst.37.17
26. Park Y, Ryu J, Ryou HS (2019) Experimental study on the fire-spreading characteristics and heat release rates of burning vehicles using a large-scale calorimeter. Energies (Basel). https://doi.org/10.3390/en12081465
27. Mowrer FW, Williamson RB (1990) Methods to characterize heat release rate data. Fire Saf J. https://doi.org/10.1016/0379-7112(90)90009-4
28. M. Goss-Sampson, *Statistical Analysis in JASP: A Guide for Students*, 6th Edition. 2024.
29. JASP Team, "JASP (Version 0.18.3)[Computer software]," 2024. [Online]. Available: https://jasp-stats.org/
30. Baker G, Wade C, Spearpoint M, Fleischmann C (2013) Developing probabilistic design fires for performance-based fire safety engineering. Procedia Eng. https://doi.org/10.1016/j.proeng.2013.08.109
31. D. Joyeux, "Natural fires in closed Car parks–Car fire tests," Metz, INC-96/294d-DJ/NB, 1997.
32. New Zealand, *Verification Method: Framework for Fire Safety Design For New Zealand Building Code Clauses C1-C6 Protection from Fire*. 2014.
33. N. Van Oerle, A. Lemaire, and P. van de Leur, (1999). Effectiveness of Forced Ventilation in Closed Car Parks.
34. Ingason H (2009) Design fire curves for tunnels. Fire Saf J. https://doi.org/10.1016/j.firesaf.2008.06.009

35. Hodges JL, Salvi U, Kapahi A (2024) Design fire scenarios for hazard assessment of modern battery electric and internal combustion engine passenger vehicles. Fire Saf J. https://doi.org/10.1016/j.firesaf.2024.104145